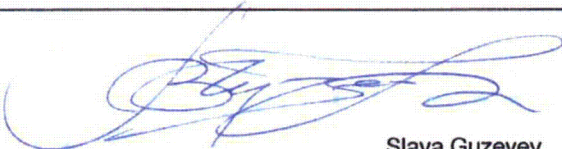
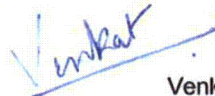
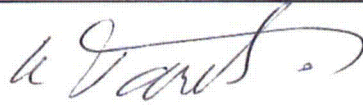
 <b>AREVA</b> TRANSNUCLEAR INC.	<b>Form 3.2-1</b> <b>Calculation Cover Sheet</b> TIP 3.2 (Revision 4)	Calculation No.:	NUH32PHB-0407
		Revision No.:	0
		Page: 1 of 20	
DCR NO (if applicable) : N/A		PROJECT NAME: NUHOMS® 32PHB System	
PROJECT NO: 10955		CLIENT: CENG - Calvert Cliff Nuclear Power Plant Inc. (CCNPP)	
<b>CALCULATION TITLE:</b>  Effective Thermal Properties of Bounding CE 14x14 Fuel Assembly for 32PHB DSC			
<b>SUMMARY DESCRIPTION:</b>  <b>1) Calculation Summary</b>  This calculation determines the effective thermal conductivity, specific heat and density for the bounding CE 14x14 fuel assembly within 32PHB DSC with helium and nitrogen backfill for use in the analysis of the thermal performance of the 32PHB DSC.  <b>2) Storage Media Description</b>  Secure network server initially, then redundant tape backup			
<b>If original issue, is licensing review per TIP 3.5 required?</b> Yes <input type="checkbox"/> No <input checked="" type="checkbox"/> (explain below)      Licensing Review No.: _____  This calculation is prepared to support a Site Specific License Application by CCNPP that will be reviewed and approved by the NRC. Therefore, a 10CFR72.48 licensing review per TIP 3.5 is not applicable.			
<b>Software Utilized (subject to test requirements of TIP 3.3):</b> ANSYS		<b>Version:</b> 10.0	
<b>Calculation is complete:</b>   Originator Name and Signature: Slava Guzeyev		4/8/2010 Date:	
<b>Calculation has been checked for consistency, completeness and correctness:</b>   Checker Name and Signature: Venkata Venigalla		4/8/2010 Date:	
<b>Calculation is approved for use:</b>   Project Engineer Name and Signature: Kamran Tavassoli		04/09/10 Date:	

## Calculation

Calculation No.: NUH32PHB-0407

Revision No.: 0

Page: 2 of 20

### REVISION SUMMARY

REV.	DESCRIPTION	AFFECTED PAGES	AFFECTED Computational I/O
0	Initial Issue	All	All



TRANSNUCLEAR INC.

## Calculation

Calculation No.: NUH32PHB-0407

Revision No.: 0

Page: 3 of 20

### TABLE OF CONTENTS

	<u>Page</u>
1.0 Purpose.....	5
2.0 Assumptions and Conservatism.....	6
3.0 Design Input.....	7
4.0 Methodology.....	8
4.1 Fuel Effective Thermal Properties.....	8
4.2 Finite Element Model.....	9
5.0 Thermal Conductivity of Irradiated Fuel .....	10
6.0 References.....	11
7.0 Computations .....	12
8.0 Results .....	14
8.1 Summary of Radial Fuel Effective Thermal Conductivity Calculation .....	16
8.2 Effective Density, Specific Heat and Axial Fuel Thermal Conductivity Evaluation ..	18
8.3 Decay Heat Load Sensitivity .....	19
9.0 Conclusion .....	20



## LIST OF TABLES

	<u>Page</u>
Table 3-1 Irradiated UO <sub>2</sub> Thermal Conductivity.....	7
Table 3-2 Zircaloy-4 Thermal Conductivity [Eq. B-2.3 of Ref.1] .....	7
Table 3-3 Nitrogen Thermal Conductivity [9].....	8
Table 5-1 Thermal Conductivity of Irradiated UO <sub>2</sub> <sup>(1)</sup> .....	10
Table 7-1 Summary of ANSYS Run .....	12
Table 7-2 List of Associated Files .....	13
Table 8-1 Radial Effective Thermal Conductivity of CE 14x14 FA in 32PHB DSC (Helium Backfill) .....	16
Table 8-2 Radial Effective Thermal Conductivity of CE 14x14 FA in 32PHB DSC (Nitrogen Backfill) .....	18
Table 8-3 Radial Effective Thermal Conductivity for Heat Load of 0.8 kW and 1.0 kW, Nitrogen Backfill .....	19
Table 9-1 Radial Effective Thermal Conductivity of Bounding CE 14x14 FA (Helium and Nitrogen Backfill).....	20

## LIST OF FIGURES

	<u>Page</u>
Figure 4-1 Finite Element Model of CE 14x14 FA.....	9
Figure 8-1 Temperature Plot for CE 14x14 FA with Helium Backfill.....	14
Figure 8-2 Temperature Plot for CE 14x14 FA with Nitrogen Backfill.....	15
Figure 8-3 Radial Effective Thermal Conductivity of CE 14x14 FA for 32PHB and 32P DSCs .....	17



## 1.0 PURPOSE

The purpose of this calculation is to determine the effective thermal conductivity, specific heat and density for the fuel assemblies (FA) within 32PHB DSC for helium and nitrogen backfill for use in the analysis of the thermal performance of the 32PHB DSC.

This calculation accounts for irradiated  $\text{UO}_2$  thermal conductivity based on [6, 7]. It also uses temperature dependent thermal conductivity of Zircaloy-4 and emissivity of fuel rod of 0.8 [1], and emissivity of stainless steel of 0.3 [3].

## 2.0 ASSUMPTIONS AND CONSERVATISM

The assumptions and conservatism from [5] are applicable to this calculation. Additional assumptions and conservatism are shown below:

1. The decay heat per fuel assembly is assumed to be 0.8 kW. Maximum decay heat per FA is 1.0 kW [4], this difference has negligible effect on FA effective thermal properties as shown in Section 8.3. The decay heat below 0.8 kW per FA also has negligible effect on FA effective thermal properties.
2. The backfill gas, fuel pellets, and water rods are not included in the axial fuel effective thermal conductivity calculation.
3. The backfill gas and water rods are not included in the effective fuel density and specific heat calculation.
4. Heat transfer in water rods is neglected.
5. The difference in dimensions between the various FA types shown in Table 4-1 of [4] is 1%, which has negligible effect on thermal analysis results. Therefore, the CE14x14 FA used as bounding for this analysis.
6. Effective thermal properties for reconstituted FA are bounded by intact FA properties. Reconstituted FA replaces number of fuel rods with stainless steel rods, reducing heat generation in FA and increasing effective thermal conductivity and specific heat of FA [10].
7. Due to small nominal fuel component dimensions its thermal expansion has negligible effect on FA geometry change and on effective thermal properties of FA.

## 3.0 DESIGN INPUT

The characteristics of the PWR fuel assemblies allowed for storage in 32PHB DSC are listed in Table 4-1 and Table 4-2 of [4]. The bounding CE14x14 FA geometry [4] is the same as that used for 32P DSC [5].

The CE14x14 FA and fuel compartment opening of 8.5 inches are identical for both 32P DSC and 32PHB DSC [5, 8].

The material properties used in 32P DSC [5] remain the same for 32PHB DSC except for following.

**Table 3-1 Irradiated UO<sub>2</sub> Thermal Conductivity**  
(See Section 5.0).

Temperature	Thermal Conductivity
°F	Btu/(hr·in·°F)
80	0.191
260	0.177
440	0.163
620	0.149
800	0.137
980	0.127
1160	0.118
1340	0.111

**Table 3-2 Zircaloy-4 Thermal Conductivity [Eq. B-2.3 of Ref.1]**

Temperature	Thermal Conductivity
°F	Btu/(hr·in·°F)
200	0.654
300	0.690
400	0.726
500	0.756
600	0.786
800	0.852



**Table 3-3 Nitrogen Thermal Conductivity [9]**

Temperature	Thermal Conductivity
°F	Btu/(hr·in·°F)
200	1.466E-03
300	1.636E-03
400	1.797E-03
500	1.950E-03
600	2.096E-03
700	2.236E-03
800	2.372E-03
900	2.503E-03
1000	2.630E-03
1100	2.753E-03

1. The emissivity of stainless steel  $\epsilon_{SS}=0.3$  is assumed based on the report [3].
2. Table B-3.11 of [1] lists the measured emissivity values for fuel cladding. For ease of calculation a bounding emissivity for Zircaloy-4 is set to  $\epsilon_{Zr-4}= 0.8$  in this calculation.

## 4.0 METHODOLOGY

### 4.1 Fuel Effective Thermal Properties

The methodology for calculating the radial, axial fuel effective thermal conductivity, density, and specific heat are the same as those used for calculating the thermal properties of bounding CE14x14 FA for storage in 32P DSC thermal analysis [5].

Using irradiated  $UO_2$  conductivity decreases the effective fuel conductivity in radial direction.

Note that as discussed in Section 4.4 of [5], the axial effective thermal conductivity is calculated

based on the fuel cladding material only and does not include the  $\text{UO}_2$  fuel pellet thermal conductivity. Therefore, the axial effective conductivity of fuel assembly is not impacted.

#### 4.2 Finite Element Model

2D finite element model of fuel assembly was developed in [5], and the current analysis is performing using ANSYS code [2].

The models were run with a series of isothermal boundary conditions applied to the nodes representing the fuel compartment walls.

The finite element model of CE 14x14 FA is shown in Figure 4-1.

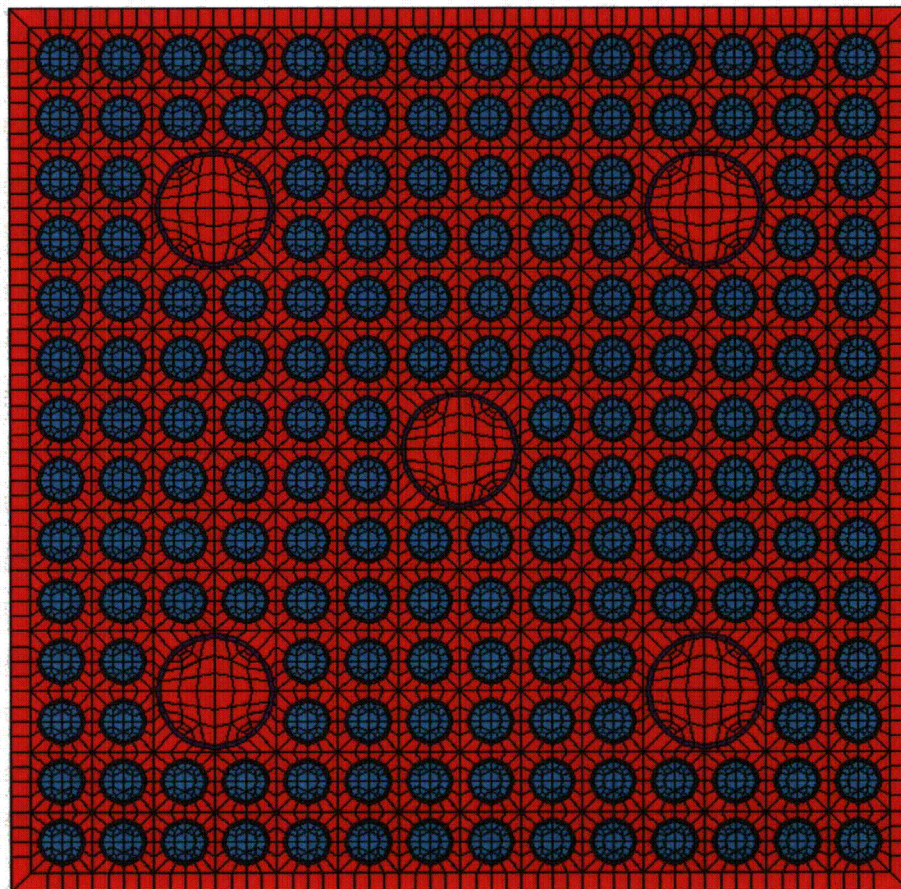


**Figure 4-1 Finite Element Model of CE 14x14 FA**



## 5.0 THERMAL CONDUCTIVITY OF IRRADIATED FUEL

The bounding thermal conductivity provided for  $UO_2$  in Section 4.1.1 of [5] is for un-irradiated  $UO_2$ . Recent data in [6] and [7] indicates potential changes in the thermal conductivity of irradiated  $UO_2$  that affects heat transfer in the fuel.

Amaya shows in [6] that the average irradiation temperature ( $T_{irr}$ ) for fuel pellet is approximately 1300 K during irradiation. This high temperature changes the characteristics of the  $UO_2$  pellets so that the thermal conductivity drops after irradiation.

The irradiated  $UO_2$  conductivity is evaluated in [7] for various irradiation temperatures from 680 to 1490 K and various burnups from 34 and 94 GWd/t. The maximum burnup of 62 GWd/t is allowed for fuel assemblies in 32PHB DSC [4]. A review of [7] shows that the thermal conductivity of irradiated  $UO_2$  with 62 GWd/t and irradiation temperature of  $T_{irr} \geq 1300K$  drops significantly (more than 50%) compared to un-irradiated  $UO_2$ .

The thermal conductivity values of irradiated  $UO_2$  are interpolated based on the data in [7] for  $T_{irr} \geq 1300$  K and burnups between 51 and 92 GWd/t for 62 GWd/t. The resultant thermal conductivity of irradiated  $UO_2$  ( $k_{UO_2}$ ) is listed in Table 5-1.

**Table 5-1 Thermal Conductivity of Irradiated  $UO_2$  <sup>(1)</sup>**

Burnup (GWd/t)	51	92	62	Interpolated values for 62 GWd/t	
Temperature (K)	$k_{UO_2}$ (W/m-K)	$k_{UO_2}$ (W/m-K)	$k_{UO_2}$ (W/m-K)	Temperature (°F)	$k_{UO_2}$ (Btu/hr-in-°F)
300	4.33	2.95	3.96	80	0.191
400	3.99	2.79	3.67	260	0.177
500	3.65	2.63	3.38	440	0.163
600	3.31	2.47	3.08	620	0.149
700	3.03	2.33	2.84	800	0.137
800	2.79	2.2	2.63	980	0.127
900	2.59	2.08	2.45	1160	0.118
1000	2.42	1.98	2.30	1340	0.111

Note (1): Interpolated data are shown in Italics.



## 6.0 REFERENCES

1. NUREG/CR-0497, *A Handbook of Materials Properties for Use in the Analysis of Light Water Reactor Fuel Rod Behavior*, MATPRO - Version 11 (Revision 2), EG&G Idaho, Inc., TREE-1280, August 1981.
2. *ANSYS On-Line User's Manual*, Version 10.0.
3. Toumas Paloposki, Leif Leidquist, *Steel Emissivity for Higher Temperatures*, Nordic Innovation Centre, NT Technical Report #570, 2006.
4. Design Criteria Document, *Design Criteria Document (DCD) for the NUHOMS 32PHB System for Storage*, Transnuclear, Inc., NUH32PHB.0101 Rev. 0.
5. Calculation, *Effective Fuel Properties*, Transnuclear, Inc., Calculation No. 1095-2, Rev. 0.
6. M. Amaya et al., "Thermal Conductivities of Irradiated  $\text{UO}_2$  and  $(\text{U,Gd})\text{O}_2$ ," *Journal of Nuclear Materials* 300 (2002) 57-64."
7. C. Ronchi et al., "Effect of Burn-up on the Thermal Conductivity of Uranium Dioxide up to 100,000  $\text{MWdt}^{-1}$ ," *Journal of Nuclear Materials* 327 (2004) 58-76.
8. Calculation, *NUHOMS<sup>®</sup> 32PHB Weight Calculation of DSC/TC System*, Calculation No. NUH32PHB-201, Rev. 0.
9. Roshenow, W. M., J. P. Hartnett, and Y. I. Cho, *Handbook of Heat Transfer*, 3<sup>rd</sup> Edition, 1998.
10. Calculation, *Effective Conductivity of the Reconfigured Fuel Assembly*, Transnuclear, Inc., Calculation No. 1095-4, Rev. 0.

## 7.0 COMPUTATIONS

The ANSYS run information is summarized in Table 7-1 below.

The runs are performed using ANSYS version 10.0 [2] with operating system Linux RedHat ES 5.1 and CPU Opteron 275 DC 2.2 GHz.

**Table 7-1 Summary of ANSYS Run**

Run Name	Date and Time	Platform	Comments
32PHB_ir1	9/04/09, 4:05 PM	Opteron 275 DC 2.2 GHz	Irradiated CE14x14 FA in helium backfill, 0.8 kW
32PHB_ir1_ni	9/16/09, 5:50 PM		Irradiated CE14x14 FA in nitrogen backfill, 0.8 kW
32PHB_ir1_ni1	10/21/09, 10:58 AM		Sensitivity run CE14x14 FA in nitrogen backfill, 1.0 kW

Associated files used in this calculation are shown in Table 7-2 below.

**Table 7-2 List of Associated Files**

File Name	Description	Date/Time
32PHB_ir1.txt	Input file for Helium backfill	7/27/09, 12:15 PM
32PHB_ir1_ni.txt	Input file for Nitrogen backfill, 0.8 kW	9/11/09, 10:38 AM
32PHB_ir1_ni1.txt	Input file for Nitrogen backfill, 1.0 kW	10/12/09, 4:57 PM
matpr-ir1_32P.txt	Material properties file (Helium backfill)	7/27/09, 12:11 PM
matpr-ir1_ni.txt	Material properties file (Nitrogen backfill)	9/4/09, 6:14 PM
mtr_ir.sub	32PHB FA radiation super-element file	9/04/09, 3:57 PM
32PHB_ir_max.txt	Maximum Temperature Results	9/04/09, 4:05 PM (helium) 9/16/09, 5:50 PM (0.8 kW, nitrogen) 10/21/09, 10:58 AM (1.0 kW, nitrogen)
Fuel.db	32P FA database for CE14x14 FA file	2/15/01 6:07 PM
Fuel.sub	32P FA radiation super-element file	2/15/01 4:07 PM
CE14_irrad_he_nitr.xls	Spreadsheet to calculate properties	9/16/09 5:59 PM
CE14_irrad_he_nitr_1.xls	Spreadsheet for sensitivity calculation	10/13/09 12:03 PM



## 8.0 RESULTS

For illustration, a temperature plot for CE 14x14 fuel assembly with 500°F applied to the compartment walls for helium and nitrogen backfill are shown in Figure 8-1 and Figure 8-2, respectively.

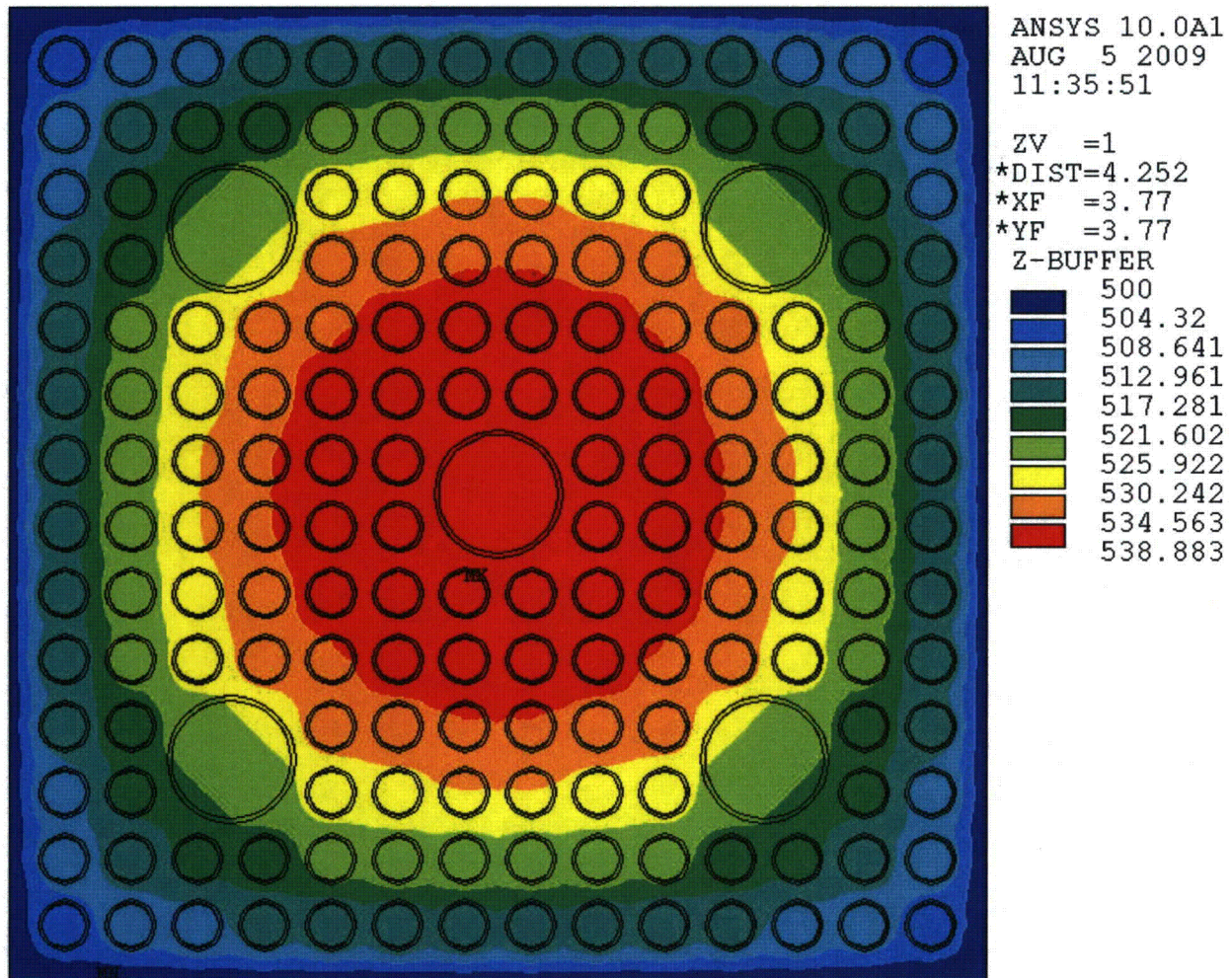
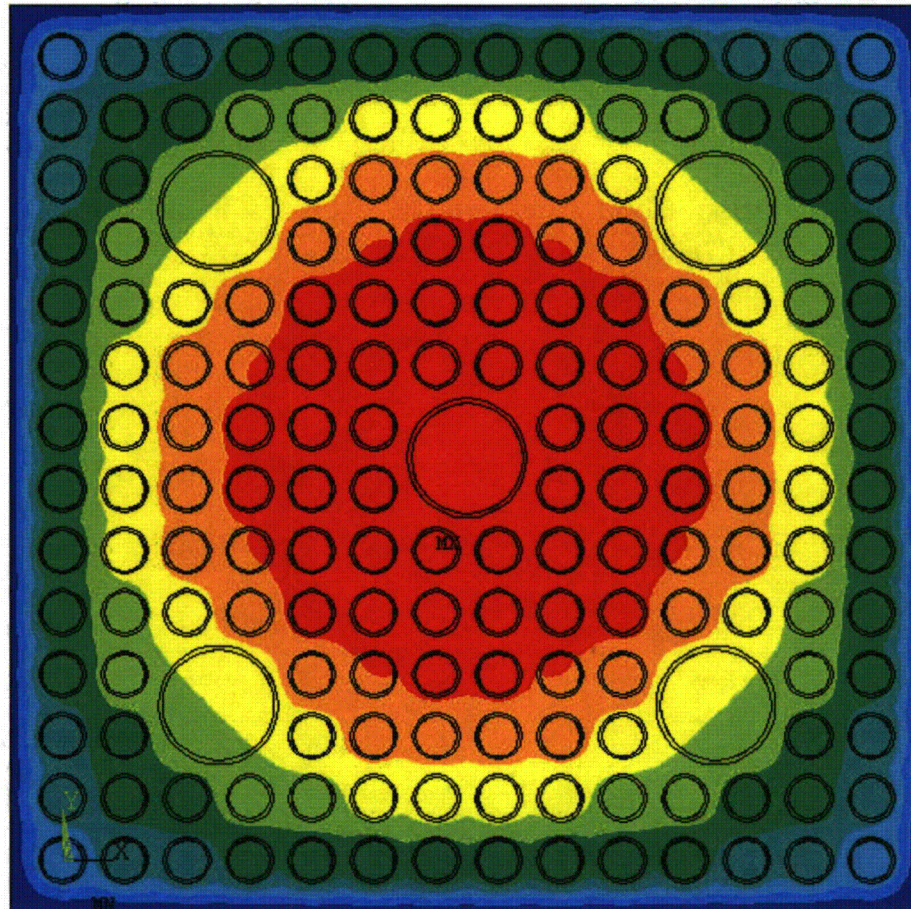


**Figure 8-1 Temperature Plot for CE 14x14 FA with Helium Backfill**





ANSYS 10.0A1  
 OCT 12 2009  
 16:41:09  
 NODAL SOLUTION  
 STEP=5  
 SUB =1  
 TIME=5  
 TEMP (AVG)  
 RSYS=0  
 PowerGraphics  
 EFACET=1  
 AVRES=Mat  
 SMN =500  
 SMX =571.789

ZV =1  
 DIST=4.675  
 XF =3.77  
 YF =3.77  
 Z-BUFFER  
 500  
 507.977  
 515.953  
 523.93  
 531.906  
 539.883  
 547.859  
 555.836  
 563.812  
 571.789

**Figure 8-2 Temperature Plot for CE 14x14 FA with Nitrogen Backfill**

## 8.1 Summary of Radial Fuel Effective Thermal Conductivity Calculation

The computed radial effective fuel thermal conductivity as function of temperature for helium backfill conditions are tabulated in Table 8-1 for irradiated CE 14x14 FA in comparison to un-irradiated CE 14x14 FA calculated for 32P DSC [5].

**Table 8-1 Radial Effective Thermal Conductivity of CE 14x14 FA in 32PHB DSC (Helium Backfill)**

32PHB DSC, irradiated CE 14x14 FA		32P DSC, un-irradiated CE 14x14 FA	
T,	k <sub>eff</sub> ,	T,	k <sub>eff</sub> ,
°F	Btu/(hr-in-°F)	°F	Btu/hr-in-°F
136	0.0202	131	0.0198
231	0.0237	226	0.0233
327	0.0277	322	0.0273
423	0.0324	419	0.0319
519	0.0378	516	0.0374
617	0.0440	614	0.0437
714	0.0508		
813	0.0583		
911	0.0665		
1010	0.0754		

The radial fuel effective thermal conductivity shown in Table 8-1 is also applicable for vacuum drying conditions if helium is used for water blow down from DSC.

Figure 8-3 provides comparison of irradiated CE 14x14 FA ( $\epsilon_{Zr-4}=0.8$ ,  $\epsilon_{SS}=0.3$ , 0.8 kW/FA) in 32PHB DSC and un-irradiated CE14x14 FA ( $\epsilon_{Zr-4}=0.6$ ,  $\epsilon_{SS}=0.587$ , 0.66 kW/FA) in 32P DSC [5].



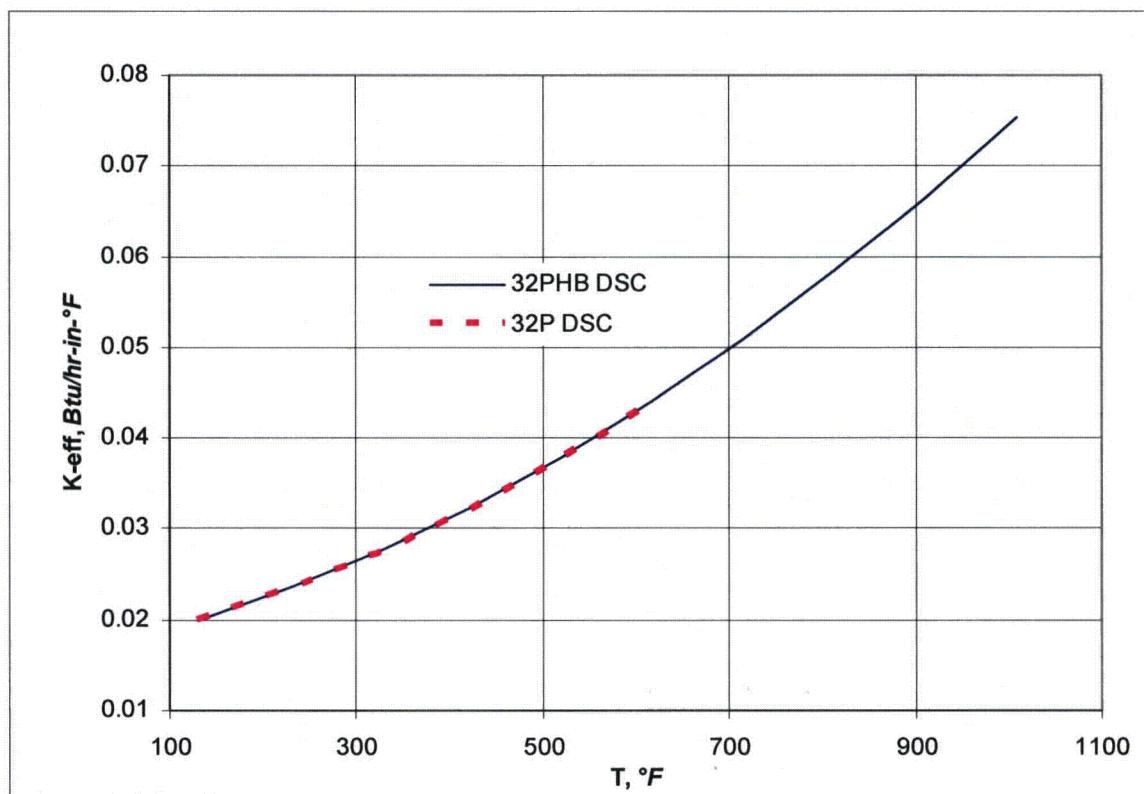


**Figure 8-3 Radial Effective Thermal Conductivity of CE 14x14 FA for 32PHB and 32P DSCs**

As seen from the above figure, the difference in radial effective thermal conductivity values between irradiated and un-irradiated FA is negligible. Values for 32PHB DSC are provided up to a temperature of 1100°F, removing additional conservatism included in 32P thermal analysis, due to limiting of temperature scale to 614°F.

The computed radial effective fuel thermal conductivity as function of temperature for nitrogen backfill conditions are tabulated in Table 8-2 for irradiated CE 14x14 FA.

**Table 8-2 Radial Effective Thermal Conductivity of CE 14x14 FA in 32PHB DSC  
(Nitrogen Backfill)**

T, °F	k <sub>eff</sub> , Btu/(hr·in·°F)
189	0.0083
271	0.0104
356	0.0131
445	0.0164
536	0.0205
629	0.0253
724	0.0310
820	0.0375
916	0.0448
1014	0.0530

The radial fuel effective thermal conductivity shown in Table 8-2 is applicable for vacuum drying conditions, if nitrogen is used for water blow down from DSC.

## 8.2 Effective Density, Specific Heat and Axial Fuel Thermal Conductivity Evaluation

Since CE 14x14 FA geometry, material density and specific heat are the same as those used in 32P DSC analysis, the density, specific heat and axial effective fuel thermal conductivity calculated for CE 14x14 FA for 32P DSC analysis [5] are applicable for 32PHB analysis and are listed below:

Effective density is  $\rho_{\text{eff FA}} = 0.1308 \text{ lbm/in}^3$  [5].

The bounding effective specific heat is  $C_{p \text{ eff FA}} = 0.0576 \text{ Btu/(lbm} \cdot \text{°F)}$  [5].

Axial fuel effective thermal conductivity is  $K_{\text{eff axial}} = 0.0601 \text{ Btu/(hr} \cdot \text{in} \cdot \text{°F)}$  [5].

## 8.3 Decay Heat Load Sensitivity

In order to show sensitivity of radial effective thermal conductivity results to the decay heat load per fuel assembly, an additional run was made for FA with nitrogen backfill and heat load of 1.0 kW.

The comparison of results for decay heat of 0.8 kW and 1.0 kW per fuel assembly is shown in Table 8-3 below.

**Table 8-3 Radial Effective Thermal Conductivity for Heat Load of 0.8 kW and 1.0 kW, Nitrogen Backfill**

	<b>0.8 kW</b>	<b>1.0 kW</b>
T, °F	$k_{eff}$ , Btu/(hr·in·°F)	$k_{eff}$ , Btu/(hr·in·°F)
300	0.0113	0.0113
400	0.0147	0.0148
500	0.0189	0.0189
600	0.0238	0.0238
700	0.0296	0.0296
800	0.0362	0.0362
900	0.0436	0.0436
1000	0.0518	0.0512

As seen from Table 8-3 the total decay heat load increase has no or negligible effect (up to 1.2 % increase) on the FA effective thermal conductivity results. Therefore, data provided for 0.8 kW decay heat load in Table 8-2 can be used for thermal analysis.



## 9.0 CONCLUSION

The radial effective thermal conductivity for bounding CE 14x14 FA for helium backfill and nitrogen backfill conditions are summarized in Table 9-1.

**Table 9-1 Radial Effective Thermal Conductivity of Bounding CE 14x14 FA  
(Helium and Nitrogen Backfill)**

Helium backfill		Nitrogen backfill	
T, °F	k <sub>eff</sub> , Btu/(hr·in·°F)	T, °F	k <sub>eff</sub> , Btu/(hr·in·°F)
136	0.0202	189	0.0083
231	0.0237	271	0.0104
327	0.0277	356	0.0131
423	0.0324	445	0.0164
519	0.0378	536	0.0205
617	0.0440	629	0.0253
714	0.0508	724	0.0310
813	0.0583	820	0.0375
911	0.0665	916	0.0448
1010	0.0754	1014	0.0530

The bounding fuel effective density is  $\rho_{\text{eff FA}} = 0.1308 \text{ lbm/in}^3$ , the bounding effective specific heat is  $C_{p \text{ eff FA}} = 0.0576 \text{ Btu/(lbm} \cdot \text{°F)}$  and the bounding axial fuel effective thermal conductivity is  $K_{\text{eff axial}} = 0.0601 \text{ Btu/(hr} \cdot \text{in} \cdot \text{°F)}$ .

Effective thermal properties for reconstituted FA are bounded by intact FA properties.